Blueprint Genetics

Retinal Dystrophy Panel Plus

REFERRING HEALTHCARE PROFESSIONAL

NAME   **HOSPITAL**

PATIENT

NAME   **DOB**   **AGE**   **GENDER**   **ORDER ID**
                                           15

PRIMARY SAMPLE TYPE   **SAMPLE COLLECTION DATE**   **CUSTOMER SAMPLE ID**

SUMMARY OF RESULTS

TEST RESULTS

The patient is heterozygous for two variants in *RPE65*:

RPE65 **c.11+5G>A, which is pathogenic.**
RPE65 **c.991_993dup, p.(Trp331dup), which is likely pathogenic.**

Del/Dup (CNV) analysis did not detect any known disease-causing copy number variation or novel or rare deletion/duplication that was considered deleterious.

PRIMARY VARIANT TABLE: SEQUENCE ALTERATIONS

GENE	TRANSCRIPT	NOMENCLATURE	GENOTYPE	CONSEQUENCE	INHERITANCE	CLASSIFICATION
RPE65	NM_000329.2	c.11+5G>A	HET	splice_region_variant, intron_variant	AR	**Pathogenic**
	ID	**ASSEMBLY** GRCh37/hg19	**POS** 1:68915573	**REF/ALT** C/T		
	gnomAD AC/AN 23/277142	**POLYPHEN** N/A	**SIFT** N/A	**MUTTASTER** N/A	**PHENOTYPE** Leber congenital amaurosis, Retinitis pigmentosa	
RPE65	NM_000329.2	c.991_993dup, p.(Trp331dup)	HET	inframe_insertion	AR	**Likely pathogenic**
	ID	**ASSEMBLY** GRCh37/hg19	**POS** 1:68904629	**REF/ALT** T/TCCA		
	gnomAD AC/AN 0/0	**POLYPHEN** N/A	**SIFT** N/A	**MUTTASTER** N/A	**PHENOTYPE** Leber congenital amaurosis, Retinitis pigmentosa	

SEQUENCING PERFORMANCE METRICS

PANEL	GENES	EXONS / REGIONS	BASES	BASES > 20X	MEDIAN COVERAGE	PERCENT > 20X
Retinal Dystrophy Panel	285	4570	905868	905355	218	99.94

TARGET REGION AND GENE LIST

The Blueprint Genetics Retinal Dystrophy Panel (version 5, Oct 19, 2019) Plus Analysis includes sequence analysis and copy number variation analysis of the following genes: ABCA4, ABCC6*, ABHD12, ACO2, ADAM9, ADAMTS18, ADGRV1, ADIPOR1*, AGBL5, AHI1, AIPL1, ALMS1*, ARHGEF18, ARL13B, ARL2BP, ARL3, ARL6, ARMC9, ARSG, ATF6, ATOH7, B9D1, B9D2, BBIP1, BBS1, BBS10, BBS12, BBS2, BBS4, BBS5, BBS7, BBS9, BEST1, C1QTNF5, C21ORF2, C2ORF71, C5ORF42, C8ORF37, CA4, CABP4, CACNA1F, CACNA2D4, CAPN5, CC2D2A#, CDH23, CDH3, CDHR1, CEP104, CEP120, CEP164, CEP19, CEP250, CEP290*, CEP41, CEP78, CERKL, CHM#, CIB2, CISD2*, CLN3, CLRN1, CNGA1#, CNGA3, CNGB1, CNGB3, CNNM4, COL11A1, COL11A2, COL18A1, COL2A1, COL9A1, COL9A2, COL9A3, CPE, CRB1, CRX, CSPP1, CTC1, CTNNA1, CTNNB1, CWC27, CYP4V2, DFNB31, DHDDS, DHX38, DRAM2, DTHD1, EFEMP1, ELOVL4, EMC1, ESPN*, EYS*, FAM161A, FDXR, FLVCR1, FRMD7, FZD4, GNAT1, GNAT2, GNB3, GNPTG, GPR179, GRK1, GRM6, GUCA1A, GUCY2D, HARS, HGSNAT, HK1#, HMX1, IDH3A, IDH3B, IFT140, IFT172, IFT27, IFT81#, IMPDH1, IMPG1, IMPG2, INPP5E, INVS, IQCB1, JAG1, KCNJ13, KCNV2, KIAA0556, KIAA0586#, KIAA0753, KIAA1549, KIF11, KIF7, KIZ, KLHL7, LCA5, LRAT, LRIT3, LRP2, LRP5*, LZTFL1, MAK, MERTK, MFN2, MFRP, MFSD8, MKKS, MKS1, MMACHC, MTTP, MVK, MYO7A, NDP, NEK2#, NMNAT1#, NPHP1, NPHP3, NPHP4, NR2E3, NR2F1, NRL, NYX, OAT, OFD1, OPA1, OPA3, OTX2, P3H2, PANK2, PAX2, PCDH15, PCYT1A, PDE6A, PDE6B, PDE6C, PDE6D, PDE6G, PDE6H, PDZD7#, PEX1, PEX10, PEX11B, PEX12, PEX13, PEX14, PEX16, PEX19, PEX2, PEX26, PEX3, PEX5, PEX6, PEX7, PHYH, PISD, PITPNM3, PLA2G5, PNPLA6, POC1B, POMGNT1, PRCD, PRDM13, PROM1, PRPF3, PRPF31, PRPF4, PRPF6, PRPF8, PRPH2, PRPS1*, RAB28, RAX2, RBP3, RBP4, RCBTB1, RD3, RDH11, RDH12, RDH5, REEP6, RGR, RGS9, RGS9BP, RHO, RIMS1, RLBP1, ROM1, RP1, RP1L1, RP2, RPE65, RPGR, RPGRIP1, RPGRIP1L#, RS1, RTN4IP1, SAG, SAMD11, SCAPER, SCLT1#, SDCCAG8, SEMA4A, SLC24A1, SLC25A46, SLC7A14, SNRNP200, SPATA7, SPP2, SRD5A3*, TCTN1#, TCTN2, TCTN3, TEAD1, TIMM8A*, TIMP3, TMEM107, TMEM126A, TMEM138, TMEM216, TMEM231, TMEM237, TMEM67, TOPORS, TRAF3IP1, TREX1, TRIM32, TRPM1, TSPAN12, TTC21B, TTC8, TTLL5, TTPA, TUB, TUBB4B, TULP1, USH1C, USH1G, USH2A, VCAN, VPS13B, WDPCP, WDR19, WFS1, YME1L1*, ZNF408, ZNF423 and ZNF513. The following exons are not included in the panel as they are not covered with sufficient high quality sequence reads: CC2D2A (NM_020785:7), CHM (NM_001145414:5), CNGA1 (NM_001142564:2), HK1 (NM_001322365:5), IFT81 (NM_031473:12), KIAA0586 (NM_001244189:6, 33), NEK2 (NM_001204182:8), NMNAT1 (NM_001297779:5), PDZD7 (NM_024895:10), RPGRIP1L (NM_015272:23), SCLT1 (NM_001300898:6) and TCTN1 (NM_001173976:2;NM_024549:6). This panel targets protein coding exons, exon-intron boundaries (± 20 bps) and selected non-coding, deep intronic variants (listed in Appendix 5). This panel should be used to detect single nucleotide variants and small insertions and deletions (INDELs) and copy number variations defined as single exon or larger deletions and duplications. This panel should not be used for the detection of repeat expansion disorders or diseases caused by mitochondrial DNA (mtDNA) mutations. The test does not recognize balanced translocations or complex inversions, and it may not detect low-level mosaicism.

*Some, or all, of the gene is duplicated in the genome. Read more: https://blueprintgenetics.com/pseudogene/
#The gene has suboptimal coverage when >90% of the gene's target nucleotides are not covered at >20x with mapping quality score (MQ>20) reads.
The sensitivity to detect variants may be limited in genes marked with an asterisk (*) or number sign (#).

CLINICAL HISTORY

Patient is a 15-year-old individual with congenital night blindness, decreased peripheral vision and pigmentary changes in the retina. Stargardt´s disease suspected. There is no family history of similar disease.

CLINICAL REPORT

Sequence analysis using the Blueprint Genetics (BpG) Retinal Dystrophy Panel identified two heterozygous variants in *RPE65*: an intronic splice region variant c.11+5G>A and an inframe insertion c.991_993dup, p.(Trp331dup). Due to the large genomic distance between these variants, NGS-based methods cannot determine whether they occur on the same (in *cis*) or different (in *trans*) parental alleles.

RPE65 c.11+5G>A

There are 23 individuals heterozygous for this variant in the Genome Aggregation Database population cohorts (gnomAD, n>120,000 exomes and >15,000 genomes). The variant affects the position 5 nucleotides downstream of the 5' donor splice site of intron 1 of *RPE65.* In silico splice prediction tools (SSF, MaxEnt, NNSPLICE, GeneSplicer, and HSF) predict that the variant will weaken or abolish the natural splice donor site and may therefore lead to aberrant splicing. The variant (referred to as 65+5G>A) was originally reported as either homozygous, or as heterozygous together with a frameshift variant in *RPE65,* in two patients with autosomal recessive retinitis pigmentosa (arRP) (PMID: 9326941). Subsequently, c.11+5G>A was reported in a compound heterozygous state with the disease-causing missense variant p.(Tyr368His) in two brothers with severe visual deficits and an absence of rod and cone electroretinographic responses before the age of 5 years. The patient's father was heterozygous for c.11+5G>A, and had good corrected visual acuity and normal visual fields. However, he was found to have subtle changes in his rod absolute dark-adapted threshold sensitivities and cone ERG flicker responses, and both his maculae were covered with hundreds of tiny hard drusen extending into the rod-rich retina beyond the macular arcades (PMID: 11786058). Subsequently, c.11+5G>A has been reported in multiple patients with Leber congenital amaurosis (LCA), arRP and retinal dystrophy (PMID: 17525851, 25257057, 28041643, 20683928, 29332120, 30268864, LOVD ID: RPE65_000058) as well as in a case of fundus albipunctatus together with the rare missense variant p.(Ile115Thr) (PMID: 21211845).

RPE65 c.991_993dup, p.(Trp331dup)

This variant is absent in the gnomAD population cohorts. The variant inserts 3 base pairs in exon 9 of *RPE65,* resulting in the inframe duplication of the tryptophan (Trp) amino acid at codon 331. *RPE65* c.991_993dup, p.(Trp331dup) has been reported in the literature to segregate with Leber congenital amaurosis in one family, in which the variant was detected as heterozygous together with a nonsense variant in *RPE65* in the index patient, and in a homozygous state in her affected aunt (PMID: 20683928). The variant has also been detected in the context of clinical testing and is submitted to ClinVar (Variation ID 658837). A disease-causing missense variant in the adjacent amino acid, p.(Cys330Tyr), has been shown in functional studies to result in a significant reduction in RPE65 isomerase activity, suggesting that this region of the protein may be functionally important (PMID: 16096063, 16150724, 24849605).

RPE65

RPE65, an abundant membrane-associated protein in the retinal pigment epithelium, is a key retinoid isomerase necessary for regenerating 11-*cis*-retinaldehyde in the visual cycle. Mice lacking RPE65 (*Rpe65*−/− and rd12) cannot synthesize 11-*cis*-retinoids; therefore photoreceptors in these mice lose light sensitivity. Pathogenic variants in *RPE65* are associated with retinal degenerative diseases such as autosomal recessive Leber congenital amaurosis, retinitis pigmentosa, and childhood onset retinal dystrophy (MIM *180069). Leber congenital amaurosis (LCA) is the earliest and most severe form of all inherited retinal dystrophies, which typically becomes evident in the first year of life (GeneReviews: http://www.ncbi.nlm.nih.gov/books/NBK1298/). The birth prevalence of LCA is two to three per 100,000 births. A number of genotype-phenotype correlations have emerged and it is extremely important to define the molecular diagnosis of the

patients due to existing targeted therapeutic options (PMID: 27102010). The prevalence of *RPE65* variants in LCA patients has been estimated at 6%-8% (PMID: 17724218, 15024725). Simonelli *et al.* showed that patients with *RPE65* variants (n=8) retain minimal visual capabilities up to 8 to 12 years and a greater integrity of retinal tissue, as shown by normal retinal thickness associated with partially preserved fundus autofluorescence. They also showed an association with night blindness. Lorenz *et al.* found that four individuals with LCA and *RPE65* pathogenic variants had measurable visual acuity at age six to ten years, despite severe visual impairment from infancy and nystagmus in three of the four (PMID: 10937591). Photophobia was not a feature and all individuals had preservation of measurable peripheral vision. Rod ERG responses were undetectable, whereas cone ERG responses were detectable in early childhood.

Thompson *et al.* screened *RPE65* in a cohort of 453 patients, of which 339 were from an unselected collection of patients with retinal dystrophy, and 114 were included on the basis of a clinical diagnosis of LCA or early-onset retinal dystrophy (PMID: 11095629). Of the latter 114 patients, 13 were found to have variants in both *RPE65* alleles (11.4%). In contrast, the *RPE65* variants accounted for 2.1% (7/339) of patients with autosomal recessive retinal dystrophy. It was concluded that *RPE65* patients share a common phenotype characterized by poor but useful visual function in early life (measurable cone ERGs) that declines dramatically throughout the school age years. In addition, a number of these patients retain residual islands of peripheral vision, although considerably compromised, into the third decade of life. Thus, the phenotype resulting from *RPE65* variants appears relatively uniform. The severity of the disease resulting from variants in *RPE65* appears to be largely independent of the variant types present in these patients.

There are 200 different disease-causing variants in the *RPE65* gene listed in the Human Gene Mutation Database (Professional 2019.3). Majority of the variants are distinct missense variants. It has been shown that the pathogenic variants eliminate the retinoid isomerase activity of RPE65. The loss of RPE65 function involves distinct mechanisms: loss of catalytic activity, a lower expression level of RPE65 or rapid degradation of the mutant protein (PMID: 16150724, 16828753).

Multiple studies have been conducted in murine and canine models of RPE65 deficiency and in human patients, in whom *RPE65* gene replacement has successfully restored cone and rod sensitivity, improved visual fields and in some cases, improved visual acuity (PMID: 27102010). The treatment is based on recombinant adeno-associated virus vector expressing RPE65 (rAAV2-CB-hRPE65). Improvement in visual function has been reported to persist for at least 3 years after treatment, however continuing retinal degeneration has been documented (PMID: 21911650, 23341635). More recent studies have reported durable benefit, but a reduction in the magnitude of improvement, after a 5- to 6-year follow-up period (PMID: 25936984). Luxturna is the first FDA approved adeno-associated virus vector-based gene therapy indicated for the treatment of patients with confirmed biallelic *RPE65* variant-associated retinal dystrophy (www.fda.gov -Luxturna).

Mutation nomenclature is based on GenBank accession NM_000329.2 (*RPE65*) with nucleotide one being the first nucleotide of the translation initiation codon ATG.

CONCLUSION

Based on the current literature and well-established role of *RPE65* c.11+5G>A, as a disease-causing variant, we classify it as pathogenic. We classify *RPE65* c.991_993dup, p.(Trp331dup) as likely pathogenic, based on the established association between the gene and the patient's phenotype, the variant's rarity in control populations, and its detection in patients with retinal dystrophy. Disease caused by *RPE65* variants is inherited in an autosomal recessive manner. Testing of parental samples is needed to determine whether the variants occur in *cis* (on the same allele) or in *trans* (on different alleles). Compound heterozygosity of the variants (variants in *trans*) would most likely explain the patient's clinical presentation. If the patient's parents are each found to be heterozygous carriers of one of these variants, then any siblings of the patient will have a 25% chance of being compound heterozygous for these variants and thus affected, a 50% chance of being an asymptomatic carrier, and a 25% chance of being an unaffected non-carrier. Genetic counseling and family member testing are recommended.

STEP   **DATE**
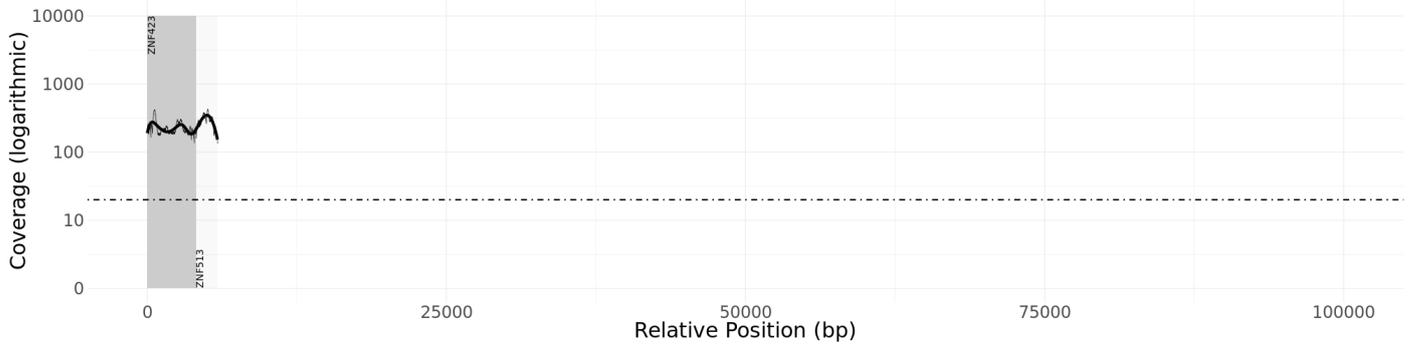
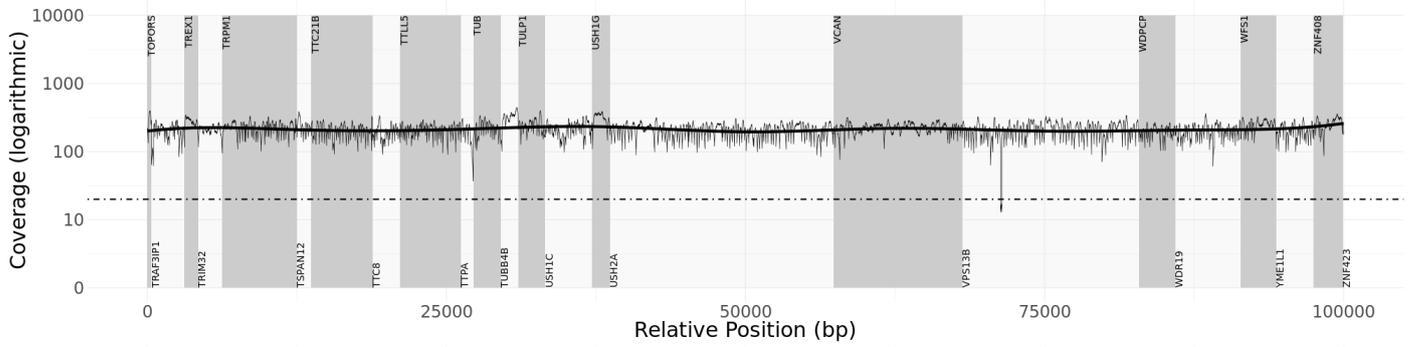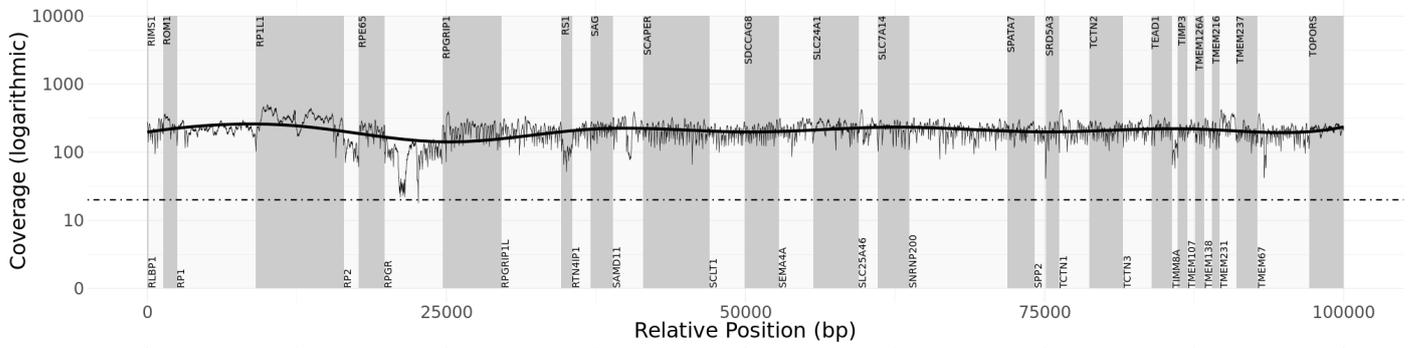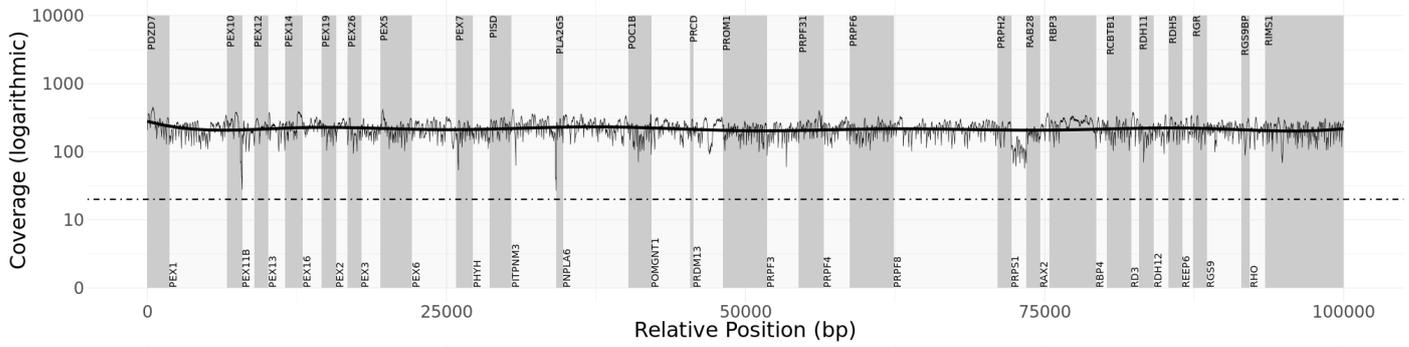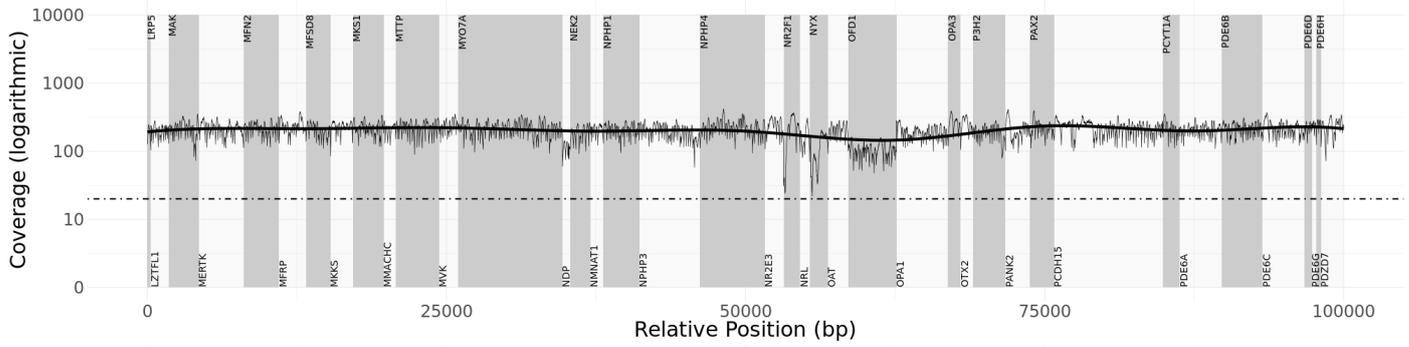| STEP	DATE
Order date	
Sample received	
Sample in analysis	
Reported	

On November 1, 2020 the statement has been prepared by our geneticists and physicians, who have together evaluated the sequencing results:

Kirsty Wells, PhD, HCPC registered clinical scientist

Senior Geneticist

Juha Koskenvuo, MD, PhD

Lab Director, Chief Medical Officer

Readability of the coverage plot may be hindered by faxing. A high quality coverage plot can be found with the full report on nucleus.blueprintgenetics.com.

APPENDIX 5: SUMMARY OF THE TEST

PLUS ANALYSIS

Laboratory process: When required, the total genomic DNA was extracted from the biological sample using bead-based method. DNA quality and quantity were assessed using electrophoretic methods. After assessment of DNA quality, qualified genomic DNA sample was randomly fragmented using non-contact, isothermal sonochemistry processing. Sequencing library was prepared by ligating sequencing adapters to both ends of DNA fragments. Sequencing libraries were size-selected with bead-based method to ensure optimal template size and amplified by polymerase chain reaction (PCR). Regions of interest (exons and intronic targets) were targeted using hybridization-based target capture method. The quality of the completed sequencing library was controlled by ensuring the correct template size and quantity and to eliminate the presence of leftover primers and adapter-adapter dimers. Ready sequencing libraries that passed the quality control was sequenced using the Illumina's sequencing-by-synthesis method using paired-end sequencing (150 by 150 bases). Base called raw sequencing data was transformed into FASTQ format. To ensure high quality of the analysis, quality control reference sample was prepared together with patient sample.

Bioinformatics and quality control: The bioinformatics analysis began with quality control of raw sequence reads. Clean sequence reads of each sample were mapped to the human reference genome (GRCh37/hg19). Burrows-Wheeler Aligner (BWA- MEM) software was used for read alignment. Duplicate read marking, local realignment around indels, base quality score recalibration and variant calling were performed using GATK algorithms (Sentieon). Variant data was annotated with public variant databases (VcfAnno, VEP). The panel content was sliced from high-quality sequencing data acquired as presented above. The sequencing depth and coverage for the tested sample was calculated based on the alignments. The sequencing run included in-process reference sample(s) for quality control, which passed our thresholds for sensitivity and specificity. The patient's sample was subjected to thorough quality control measures as well, after which raw sequence reads were transformed into variants by a proprietary bioinformatics pipeline. Copy number variations (CNVs), defined as single exon or larger deletions or duplications (Del/Dups), were detected from the sequence analysis data using a proprietary bioinformatics pipeline, which processes aligned sequence reads. The difference between observed and expected sequencing depth at the targeted genomic regions was calculated and regions were divided into segments with variable DNA copy number. The expected sequencing depth was obtained by using other samples processed in the same sequence analysis as a guiding reference. The sequence data was adjusted to account for the effects of varying guanine and cytosine content.

Interpretation: Our variant classification follows the Blueprint Genetics Blueprint Genetics Variant Classification Schemes modified from the ACMG guideline 2015. Minor modifications were made to increase reproducibility of the variant classification and improve the clinical validity of the report. Likely benign and benign variants were not reported. The pathogenicity potential of the identified variants were assessed by considering the predicted consequence, the biochemical properties of the codon change, the degree of evolutionary conservation as well as the number of reference population databases and mutation databases such as, but not limited to, the gnomAD, ClinVar, HGMD Professional and Alamut Visual. For missense variants, *in silico* variant prediction tools such as SIFT, PolyPhen, MutationTaster were used to assist with variant classification. In addition, the clinical relevance of any identified CNVs was evaluated by reviewing the relevant literature and databases such as Database of Genomic Variants, ExAC, gnomAD and DECIPHER. The clinical evaluation team assessed the pathogenicity of the identified variants by evaluating the information in the patient referral, reviewing the relevant literature and manually inspecting the sequencing data if needed. Reporting was carried out using HGNC-approved gene nomenclature and mutation nomenclature following the HGVS guidelines.

Confirmation: Pathogenic and likely pathogenic variants that established a molecular diagnosis were confirmed with bi-directional Sanger sequencing unless the following criteria were fulfilled: 1) the variant quality score (QS) was above the internal threshold for a true positive call and 2) visual check-up of the variant at IGV is in-line with the variant call. Reported variants of uncertain significance were confirmed with bi-directional Sanger sequencing only if the QS was below our internally defined score for a true positive call. CNVs (Dels/Dups) were confirmed using a quantitative-PCR assay if they covered less than 10 exons (heterozygous), less than 3 exons (homo/hemizygous) or were not confirmed at least three times previously at our laboratory.

Analytic validation: This laboratory-developed test has been independently validated by Blueprint Genetics. The sensitivity of this panel is expected to be in the same range as the validated next generation sequencing assay used to generate the panel data (sensitivity for SNVs 99.9%, indels 11-50 bps 99.1%, one-exon deletions 100% and 1-9 exon duplications 75%, and specificity >99.9% for most variant types). It does not detect very low-level mosaicism as a variant with minor allele fraction of 14.6% can be detected in 90% of the cases.

Test restrictions: A normal result does not rule out the diagnosis of a genetic disorder since some DNA abnormalities may be undetectable by the applied technology. Test results should always be interpreted in the context of clinical findings, family history, and other relevant data. Inaccurate, or incomplete information may lead to misinterpretation of the results.

Regulation and accreditations: This test has not been cleared or approved by the FDA. This analysis has been performed in a CLIA-certified laboratory (#99D2092375) and accredited by the College of American Pathologists (CAP #9257331). All the tests are under the scope of the ISO 15189 accreditation (excluding mtDNA testing and digital PCR confirmation).

NON-CODING VARIANTS COVERED BY THE PANEL:

NM_000350.2(ABCA4):c.6730-19G>A
NM_000350.2(ABCA4):c.6148-471C>T
NM_000350.2(ABCA4):c.5197–557G>T
NM_000350.2(ABCA4):c.5196+1137G>A
NM_000350.2(ABCA4):c.5196+1056A>G
NM_000350.2(ABCA4):c.4539+2065C>G
NM_000350.2(ABCA4):c.4539+2064C>T
NM_000350.2(ABCA4):c.4539+2028C>T
NM_000350.2(ABCA4):c.4539+2001G>A
NM_000350.2(ABCA4):c.4539+1928C>T
NM_000350.2(ABCA4):c.4539+1729G>T
NM_000350.2(ABCA4):c.4539 +1106C>T
NM_000350.2(ABCA4):c.4539+1100A>G
NM_000350.2(ABCA4):c.4253+43G>A
NM_000350.2(ABCA4):c.3191–11T>A
NM_000350.2(ABCA4):c.3051-16T>A
NM_000350.2(ABCA4):c.3050+370C>T
NM_000350.2(ABCA4):c.2919-383C>T
NM_000350.2(ABCA4):c.2160+584A>G
NM_000350.2(ABCA4):c.1938-619A>G
NM_000350.2(ABCA4):c.1937+435C>G
NM_000350.2(ABCA4):c.1937+13T>G
NM_000350.2(ABCA4):c.859-506G>C
NM_000350.2(ABCA4):c.859–540C>G
NM_000350.2(ABCA4):c.769–784C>T
NM_000350.2(ABCA4):c.768+3223C>T
NM_000350.2(ABCA4):c.570+1798A>G
NM_000350.2(ABCA4):c.302+68C>T
NM_000350.2(ABCA4):c.161–23T>G
NM_000350.2(ABCA4):c.67-16T>A
NM_001171.5(ABCC6):c.4403+11C>G
NM_001171.5(ABCC6):c.3506+15G>A
NM_001171.5(ABCC6):c.1780-29T>A
NM_001171.5(ABCC6):c.1432-22C>A
NM_024649.4(BBS1):c.951+58C>T
NM_033028.4(BBS4):c.77-216delA
NM_152384.2(BBS5):c.619-27T>G
NM_001139443.1(BEST1):c.-29+1G>T
NM_001139443.1(BEST1):c.-29+5G>A
NM_001271441.1(C21ORF2):c.1000-23A>T
NM_025114.3(CEP290):c.6012-12T>A
NM_025114.3(CEP290):c.2991+1655A>G
NM_025114.3(CEP290):c.1910-11T>G
NM_025114.3(CEP290):c.103-18_103-13delGCTTTT
NM_000390.2(CHM):c.315-1536A>G

NM_000390.2(CHM):c.315-4587T>A
chrX:g.85302626-85302626
chrX:g.85302634-85302634
chrX:g.85302634-85302634
chrX:g.85302644-85302644
NM_000086.2(CLN3):c.1056+34C>A
NM_000086.2(CLN3):c.461-13G>C
NM_001195794.1(CLRN1):c.254-649T>G
NM_001298.2(CNGA3):c.-37-1G>C
NM_080629.2(COL11A1):c.3744+437T>G
NM_080629.2(COL11A1):c.1027-24A>G
NM_080629.2(COL11A1):c.781-450T>G
NM_001844.4(COL2A1):c.1527+135G>A
NM_024887.3(DHDDS):c.441-24A>G
NM_001142800.1(EYS):c.-448+5G>A
NM_194277.2(FRMD7):c.285-118C>T
NM_005272.3(GNAT2):c.461+24G>A
NM_032520.4(GNPTG):c.610-16_609+28del
NM_000180.3(GUCY2D):c.-9-137T>C
NM_152419.2(HGSNAT):c.821-28_821-10delTTGCTTATGCTTTGTACTT
NM_033500.2(HK1):c.-390-3838G>C
NM_033500.2(HK1):c.-390-3818G>C
NM_033500.2(HK1):c.27+14901A>G
NM_014714.3(IFT140):c.2577+25G>A
NM_000214.2(JAG1):c.1349-12T>G
NM_004744.3(LRAT):c.541-15T>G
NM_000253.2(MTTP):c.619-5_619-2delTTTA
NM_000253.2(MTTP):c.1237-28A>G
NM_000431.2(MVK):c.769-7dupT
NM_000260.3(MYO7A):c.-48A>G
NM_000260.3(MYO7A):c.3109-21G>A
NM_000260.3(MYO7A):c.5327-14T>G
NM_000260.3(MYO7A):c.5327-11A>G
NM_000260.3(MYO7A):c.5857-27_5857-26insTTGAG
NM_000266.3(NDP):c.-207-1G>A
NM_000266.3(NDP):c.-208+5G>A
NM_000266.3(NDP):c.-208+2T>G
NM_000266.3(NDP):c.-208+1G>A
NM_000266.3(NDP):c.-343A>G
NM_000266.3(NDP):c.-391_-380delCTCTCTCTCCCTinsGTCTCTC
NM_000266.3(NDP):c.-396_-383delTCCCTCTCTCTCTC
NM_022787.3(NMNAT1):c.-70A>T
NM_022787.3(NMNAT1):c.-69C>T
NM_022787.3(NMNAT1):c.-57+7T>G
NM_003611.2(OFD1):c.935+706A>G
NM_003611.2(OFD1):c.1130-22_1130-19delAATT
NM_003611.2(OFD1):c.1130-20_1130-16delTTGGT
NM_130837.2(OPA1):c.449-34dupA
NM_130837.2(OPA1):c.2179-40G>C
NM_153638.2(PANK2):c.*40G>C
NM_001142763.1(PCDH15):c.-29+1G>C
NM_006204.3(PDE6C):c.481-12T>A
NM_000287.3(PEX6):c.2301-15C>G
NM_000287.3(PEX6):c.2300+28G>A
NM_000288.3(PEX7):c.-45C>T

chr6:g.100040906-100040906
chr6:g.100040987-100040987
chr6:g.100041040-100041040
NM_021620.3(PRDM13):c.-8128A>C
NM_021620.3(PRDM13):c.-8107T>C
NM_006017.2(PROM1):c.2077-521A>G
NM_015629.3(PRPF31):c.1073+20_1073+36delCGGTAGGCATGGGGGTC
NM_015629.3(PRPF31):c.1374+654C>G
chr9:g.116037909-116037909
NM_002905.3(RDH5):c.-33+2dupT
NM_000329.2(RPE65):c.246-11A>G
chrX:g.38128234-38128234
NM_001034853.1(RPGR):c.1059+363G>A
NM_020366.3(RPGRIP1):c.1468-263G>C
NM_020366.3(RPGRIP1):c.1611+27G>A
NM_020366.3(RPGRIP1):c.2367+23delG
NM_020366.3(RPGRIP1):c.2367+23delG
NM_020366.3(RPGRIP1):c.2711-13G>T
NM_004085.3(TIMM8A):c.133-23A>C
NM_001077416.2(TMEM231):c.824-11T>C
NM_206933.2(USH2A):c.14583-20C>G
NM_206933.2(USH2A):c.9959-4159A>G
NM_206933.2(USH2A):c.8845+628C>T
NM_206933.2(USH2A):c.7595-2144A>G
NM_206933.2(USH2A):c.5573-834A>G
NM_206933.2(USH2A):c.486-14G>A
NM_206933.2(USH2A):c.-259G>T
NM_006005.3(WFS1):c.-43G>T

GLOSSARY OF USED ABBREVIATIONS:

AD = autosomal dominant

AF = allele fraction (proportion of reads with mutated DNA / all reads)

AR = autosomal recessive

CNV = Copy Number Variation, eg, one exon or multiexon deletion or duplication

gnomAD = genome Aggregation Database (reference population database; >138,600 individuals)

gnomAD AC/AN = allele count/allele number in the genome Aggregation Database (gnomAD)

HEM = hemizygous

HET = heterozygous

HOM = homozygous

ID = rsID in dbSNP

MT = Mitochondria

MutationTaster = *in silico* prediction tools used to evaluate the significance of identified amino acid changes.

Nomenclature = HGVS nomenclature for a variant in the nucleotide and the predicted effect of a variant in the protein level

OMIM = Online Mendelian Inheritance in Man®

PolyPhen = *in silico* prediction tool used to evaluate the significance of amino acid changes.

POS = genomic position of the variant in the format of chromosome:position

SIFT = *in silico* prediction tool used to evaluate the significance of amino acid changes.